

Wavelet Transform Analysis of Pressure Fluctuation Signals in a Three-Phase Fluidized Bed

Soung Hee Park[†] and Sang Done Kim^{*}

Department of Chemical Engineering, Woosuk Univ., Chonbuk 565-701, Korea

^{*}Department of Chemical Engineering, Korea Advanced Institute of Science and Technology, Daejeon 305-701, Korea

(Received 10 April 2001 • accepted 23 July 2001)

Abstract—The wavelet transform based on localized wavelet functions is applicable to analysis of pressure fluctuation signals from different flow regimes of a three-phase fluidized bed, which usually is nonlinear or nonstationary. The pressure fluctuation has been analyzed by resorting to the discrete wavelet transform such as wavelet coefficients, wavelet energy, and time-scale plane. The dominant scale of wavelet coefficients and the highest wavelet energy in the bubble-disintegrating regime are finer than ones in the bubble-coalescence regime. The cells corresponding to fine scale of time-scale plane in bubble-disintegrating regime are more shaded and energetic, while the cells corresponding to coarse scale in bubble-coalescence regime are more energetic. Therefore, the wavelet transform enables us to obtain the frequency content of objects in a three-phase fluidized bed locally in time.

Key words: Wavelet Transform, Fourier Transform, Three-Phase Fluidized Bed, Pressure Fluctuation, Flow Regime

INTRODUCTION

Three-phase fluidized beds have been adopted widely for various chemical, pharmaceutical and biochemical systems as reactors, contactors and separation units since they exhibit high heat and mass transfer rates due to efficient contact between the phases during continuous operation [Fan, 1989; Kang et al., 1999]. Since the heat and mass transfer as well as hydrodynamic properties such as phase hold-up and bed porosity, bubble properties, and mixing characteristics show very different characteristics as the flow regime changes, many authors have studied the flow regime transition in three-phase fluidized beds. The identification of flow regime is a fundamental basis of fluid dynamic analysis for reactor modeling. However, the lack of more complete knowledge of the three-phase fluidized bed fluid dynamic behavior causes several operational difficulties and design uncertainties. Therefore, several investigators [Han, 1990; Han and Kim, 1993; Kwon et al., 1994] have examined the bubble properties and its flow behavior by analysis of pressure fluctuations obtained from the three-phase fluidized bed.

The characteristics of the pressure fluctuations have been studied by several analysis methods such as statistical analysis, Fourier transform and deterministic chaos analysis based on fractional Brownian motion [Park, 1989; Kwon et al., 1994; Kim and Han, 1999; Lee et al., 2001]. The Fourier transform and its inverse establish a one-to-one relation between the time domain and the frequency domain, which is a classical analysis tool widely used. This transform uses sine and cosine as its bases to map a time domain function into frequency domain. Thus, the spectrum shows the global strength with which any frequency is contained in the function. However, the Fourier transform does not show how the frequencies vary with time in the spectrum. Nevertheless, time-varying frequencies are

quite common in natural phenomena, e.g., seismic signals and nonstationary geophysical process [Farge, 1992; Wornell, 1993]. To investigate such phenomena, we need a transform that enables us to obtain the frequency content of a process locally in time.

Wavelet analysis is an emerging field that has provided new tools and algorithms suited for the types of problems encountered in signal processing and process monitoring. In wavelet analysis, we can use linear combinations of wavelet functions to represent signals. Some characteristics which make the wavelet approximations remarkable and useful are: wavelets are localized in time and are good building block functions for a variety of signals, including signals with features which change over time and signals which have jumps and other non-smooth features.

In this study, we applied both Fourier transform and wavelet transform to pressure fluctuation signals in different flow regimes of a three-phase fluidized bed, and then compared the two techniques. We proposed the wavelet transform as a new alternative tool for identification of bed properties in three-phase fluidized bed reactor.

THEORETICAL

In this section, only a brief introduction to Fourier transform and wavelet transform is provided. The interested reader may refer to the referenced review articles and books for further details [Otnes and Enochson, 1978; Chui, 1992; Motard and Joseph, 1994; Wickhauser, 1994; Mallat, 1998].

The aim of signal analysis is to extract relevant information from a signal by transforming it. The natural stationary transform is the well-known Fourier transform. The analysis coefficients $X(f)$ define the notion of global frequency f in a signal. As shown in Eq. (1), they are computed as inner products of the signal with sine-wave basis functions of infinite duration.

$$\hat{X}(f) = \int_{-\infty}^{\infty} X(t) e^{-j2\pi ft} dt = \int_{-\infty}^{\infty} X(t) [\cos(2\pi ft) - j\sin(2\pi ft)] dt \quad (1)$$

[†]To whom correspondence should be addressed.

E-mail: drpark@woosuk.ac.kr

The Fourier transform yields the energy density in an individual frequency range. As can be seen in power spectrum of a time series, the Fourier basis function is localized only in the frequency but not in time because the estimation is performed throughout the time series. Moreover, a coefficient with a small value would be masked by other coefficients with large values.

Wavelets are a new family of localized basis functions that have found many applications in quite a large area of science and engineering [Motard and Joseph, 1994; Mallat, 1998]. Wavelets, or analyzing wavelets, are the building blocks of wavelet transforms, just as trigonometric functions of different frequencies are the building blocks used in Fourier transforms. Wavelets are generated by the dilation and the translation of a single prototype function called the mother wavelet. The mother wavelet is an absolutely integrable function and is denoted as $\Psi(t)$. Performing scaling and translation operations on this mother wavelet $\Psi(t)$ creates a family of scaled and translated versions of the mother wavelet function. Thus, the family of functions defined by

$$\Psi_{a,b}(t) = |a|^{-1/2} \Psi\left(\frac{t-b}{a}\right) \quad (2)$$

where $a, b \in \mathbb{R}$ and $a \neq 0$, are wavelets; a is called the dilation parameter, and b the translation parameter. The scaling operation of the mother wavelet can be used to catch the different frequency information of the function to be analyzed. The "compressing" version is used to fit the high frequency needs, and the "stretching" version is for low frequency requirements. The translation operation, on the other hand, involves "shifting" of the mother wavelet along the time axis. Then the translated version is used to catch the time information of the function to be analyzed. In this way, a family of scaled and translated wavelets is created according to the different scaling and translation parameters a and b , which serve as the base, the building blocks, for representing the function to be analyzed.

Like Fourier transforms, where a function is projected onto trigonometric functions with different frequencies, the wavelet transform projects a function onto analyzing functions with different dilation and translation parameters. The wavelet transform maps a time domain function onto the two-dimensional time-scale domain. The wavelet transform involves computation of the inner products between the function and the wavelets. The inner products are called the wavelet coefficients and are defined as:

$$\langle f(t), \Psi_{a,b}(t) \rangle = |a|^{-1/2} \int_{-\infty}^{\infty} f(t) \Psi\left(\frac{t-b}{a}\right) dt \quad (3)$$

EXPERIMENTS

The experimental facilities, shown in Fig. 1, consisted of an assembly of a three-phase fluidized bed, a measuring assembly, and a calculating/recording assembly. All experiments were performed in a Plexiglas column at room temperature ($25^\circ \pm 1^\circ \text{C}$) under atmospheric pressure. The column inside diameter was 0.376 m, and its height was 2.1 m. A perforated plate with 786 evenly spaced holes, 3 mm in diameter, served as the liquid distributor. Air was fed to the column through a grid of feed pipes, each with an inside diameter of 6.4 mm; the grid was provided with 232 horizontally drilled holes, 1 mm in diameter. Pressure taps to measure the static pressure with a liquid manometer were mounted flush along the

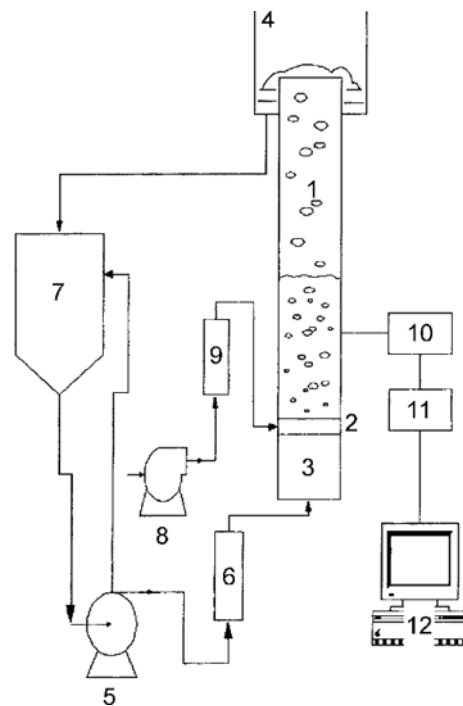


Fig. 1. Schematic diagram of experimental apparatus.

1. Main column	7. Liquid reservoir
2. Distributor	8. Air compressor
3. Calming section	9. Flowmeter
4. Weir	10. Pressure transducer
5. Pump	11. Data acquisition system
6. Flowmeter	12. PC

wall of the column; they were axially distributed, and the distance between any pair of adjacent taps was 0.14 m. The fluidizing liquid and gas were water and oil-free compressed air, respectively. The fluidized solid was spherical glass beads with a density of $2,500 \text{ kg/m}^3$. They had a diameter of 1.0 mm, 2.3 mm and 6.0 mm, respectively. The pressure tap for measuring pressure fluctuations was located at 0.4 m above the distributor. The differential pressure transducer generated an output voltage proportional to the pressure fluctuation signal. The signal was stored in a data acquisition system (Data Precision Model, D-6000) and processed by a personal computer.

In each experimental run, the particles were suspended in the bed by the fluidized gas at a flow rate within the range between 0 and 0.10 m/s, and the fluidized liquid at a flow rate within the range between 0 and 0.10 m/s. Once a steady state was reached, the fluctuating voltage-time signals, corresponding to the fluctuating pressure-time signals, from the differential pressure transducer were sampled at a rate of 0.01 s and stored in the data acquisition system. The overall data acquisition time was 41 s, thereby yielding a total of 4100 data points. The signals were transmitted to the computer. Wavelet transform of the pressure fluctuation using the S⁺Wavelet software (MathSoft Inc.) was calculated from the digitized data acquired. We used Coifman wavelet as mother wavelet.

RESULT AND DISCUSSION

Typical pressure fluctuations at different flow regimes, bubble-coalescence regime and bubble-disintegrating regime, in a three-

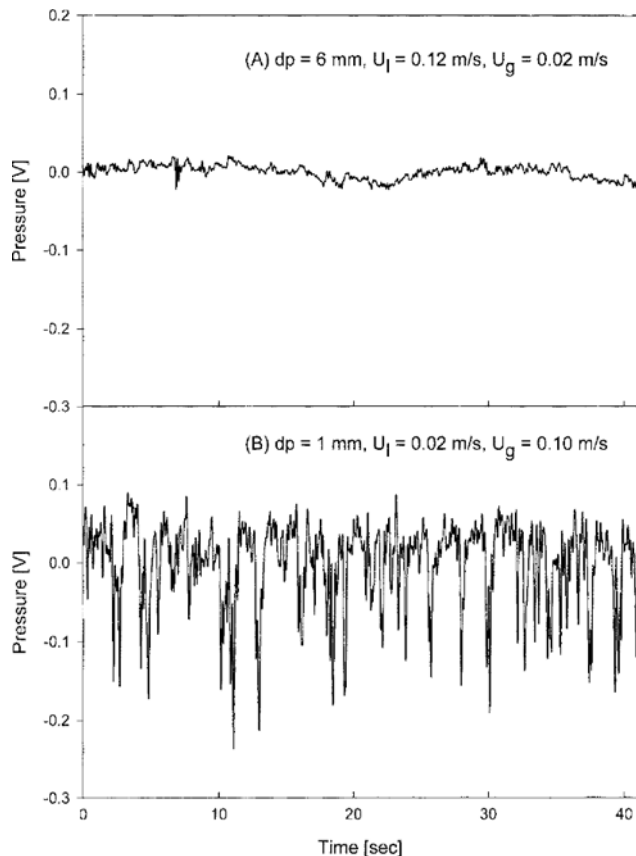


Fig. 2. Typical pressure fluctuation signals at different flow regimes, (A) bubble-disintegrating regime (B) bubble-coalescence regime.

phase fluidized bed are shown in Fig. 2. As can be seen, it fluctuates very randomly over the entire experiment time. Through the signals for these pressure fluctuation signals with time we might know the difference of amplitude of the signals between bubble-coalescence regime and bubble-disintegrating regimes. But we cannot recognize the existence and movement of the objects in the bed. Thus, it is difficult to classify into the flow regimes by this pressure time signals. Therefore, to get some information about properties of pressure fluctuation in frequency domain, many researchers have calculated a power spectral density function using a Fourier transform.

The power spectral density functions of pressure fluctuation in three-phase fluidized beds are calculated and presented in Fig. 3. A peak or peaks in the spectrum correspond, respectively, to a major periodic component or components in the random variable [Lee and Kim, 1988; Park, 1989]. Note that in Fig. 3, a distinct peak appears between 0 and 10 Hz in the power spectra. These peaks indicate the existence of corresponding objects of the frequencies, usually, bubbles. The Fourier transform yields the energy density in an individual frequency. As shown in this figure, the major peaks move to lower frequency in the bubble-coalescence regime than in the bubble-disintegrating regime. Since the bubble coalescing may be enhanced in the bubble-coalescence regime, the bubble size is bigger in the bubble-coalescence regime than in the bubble-disintegrating regime [Han, 1990; Kim and Kang, 1996]. It is known that the bigger the bubble size, the lower the peak in a power spectrum.

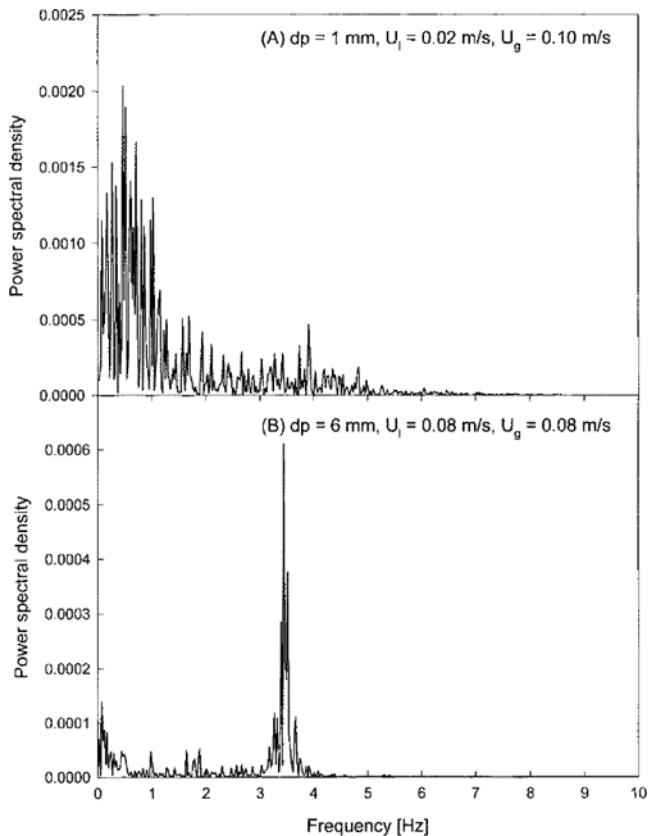


Fig. 3. Power spectra obtained from Fourier transform at different flow regimes, (A) bubble-coalescence regime (B) bubble-disintegrating regime.

However, the Fourier basis function is localized only in the frequency but not in time. Even though the spectral density function indicates that the major frequency is generated by bubbles, it cannot reveal the movement of those bubbles in the bed over time. This is a disadvantage of the Fourier transform, which is unable to permit time localization.

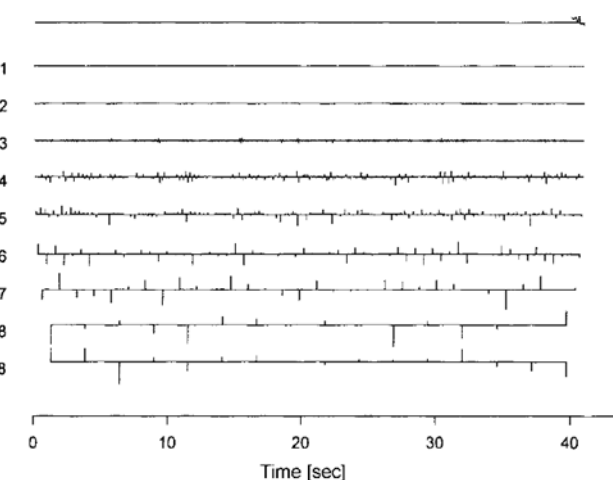


Fig. 4. Plot of coefficients of discrete wavelet transform of a pressure fluctuation signal at a bubble-disintegrating flow regime.

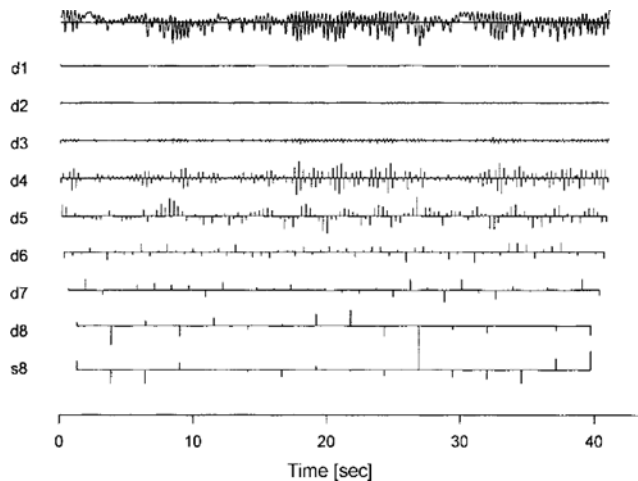


Fig. 5. Plot of coefficients of discrete wavelet transform of a pressure fluctuation signal at a bubble-coalescence flow regime.

The coefficients of discrete wavelet transform (DWT) of pressure fluctuation at different regimes are computed and plotted in Figs. 4 and 5, respectively. The original signal is plotted in the top row. The wavelet coefficients are plotted in the remaining rows, going from the fine scale d_1 coefficients in the second row to the coarse scale coefficients d_2 and s_2 in the bottom two rows. The coefficients are plotted as vertical lines extending from zero. The fine scale features (the high frequency oscillations) are captured mainly by the fine scale detail components d_1 and d_2 . The coarse scale components d_2 and s_2 correspond to lower frequency oscillations, that is, large bubbles. In Fig. 4 the dominant scale in the over the experiment time is d_4 scale, which is finer than d_1 in Fig. 5 in bubble-coalescence regime. Thus, this can indicate that the bed in the bubble-disintegrating regime has a smaller bubble than in the bubble-coalescence regime. Also, from the change of the pattern over the time we may estimate the passage of the bubbles in the three-phase fluidized beds. Therefore, it is available for knowing the change of bed properties of three-phase fluidized bed such as bubble phenomena over the time.

The wavelet energy, which is the percentage of energy of the analyzed signal over scales obtained from coefficient of discrete wavelet transform, is shown in Fig. 6. The wavelet energy is defined as follows:

$$E_j^2 = \frac{1}{E} \sum_{k=1}^{n^2} d_{j,k}^2, j=1, \dots, J \quad (4)$$

$$E_j^2 = \frac{1}{E} \sum_{k=1}^{n^2} s_{j,k}^2 \quad (5)$$

where $E = \sum_{k=1}^{n^2} f_k^2$ is the total energy of the signal. In Fig. 6 the scale of the highest wavelet energy is moved from fine scale to coarse scale as the change of major frequency in power spectrum from Fourier transform.

The time-scale plot produces an easily interpretable visual two-dimensional representation of signals, where each pattern in the time-scale plane contributes to the global energy of the signal. The time-scale plane is defined as the squared modulus of the wavelet transform [Rioul and Vetterli, 1991]. As can be seen in Figs. 7 and 8,

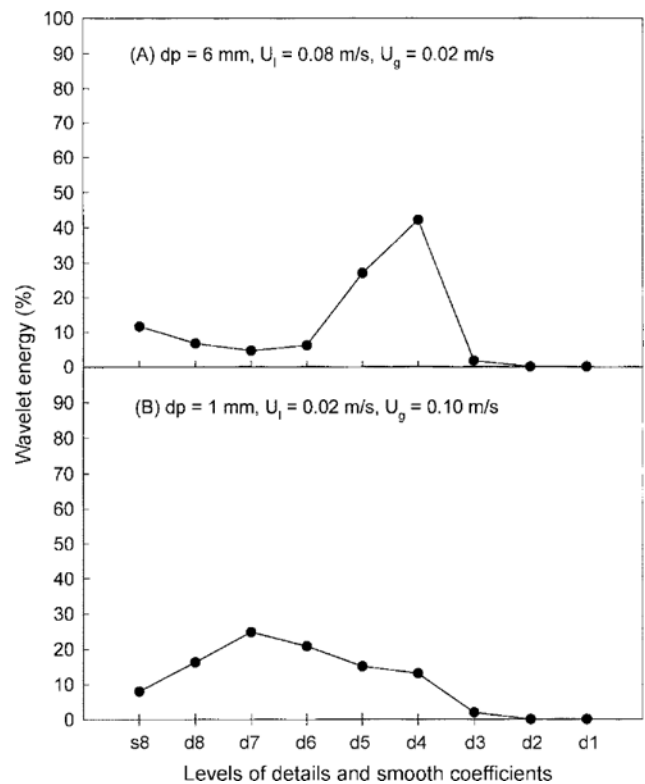


Fig. 6. Wavelet energy distribution of the pressure fluctuation signals at different flow regimes, (A) bubble-disintegrating regime (B) bubble-coalescence regime.

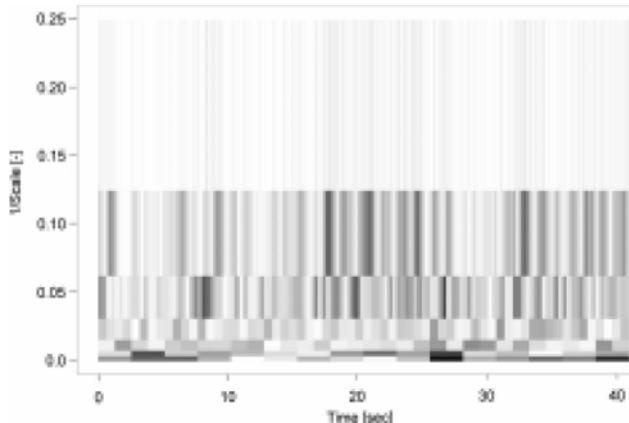


Fig. 7. Time-scale plane of the pressure fluctuation signal at a bubble-disintegrating flow regime.

time-scale planes of the pressure signal are obtained at different flow regimes, respectively. In these figures, the x axis represents time, while the y axis represents $1/\text{scale}$ and ranges from 0 (coarsest scale) to 1 (finest scale). The level of energy of an individual time-scale cell is indicated as a shade of gray. The darker the cell, the higher the energy content of the time-scale cell. The cells corresponding to fine scale are more shaded and energetic in Fig. 7, while the cells corresponding to coarse scale are more energetic in Fig. 8. It is known that the bed in the bubble-coalescence regime has bigger bubbles than in the bubble-disintegrating regime. Thus, the more often the bubble coalescence, the greater the energy content of cells in the

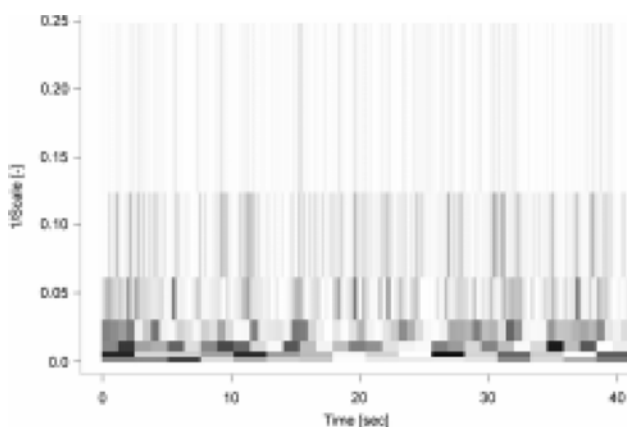


Fig. 8. Time-scale planes of the pressure fluctuation signals at a bubble-coalescence flow regime.

coarse scale range in the bubble-coalescence regime. This is consistent with the result from evaluation of the power spectrum by Fourier transform. Also, these figures show that the cells change over time. It means that the time-scale plane obtained by wavelet transform provides both the localization of scale and time, and makes it possible to identify the status of the bed such as passage of bubbles.

CONCLUSIONS

The pressure fluctuations at different flow regimes in a three-phase fluidized bed have been analyzed using the wavelet transform analysis: the time series of pressure fluctuation signals have been analyzed by means of wavelet transform coefficients, wavelet energy and time-scale plane. The dominant scale of wavelet coefficients and the highest wavelet energy in the bubble-disintegrating regime are finer than ones in the bubble-coalescence regime. Time-scale plane shows the different pattern of the objects with frequency and time domain at different bubble flow regimes. Therefore, wavelet transform enable us to obtain the frequency content of objects in a three-phase fluidized bed locally in time. These are useful tools to identify the status of bed in the three-phase fluidized bed. Consequently, the wavelet transform is expected to be useful for analyzing the pressure fluctuation signals to understand the hydrodynamics in a three-phase fluidized bed.

ACKNOWLEDGEMENT

This research was supported by Woosuk University.

NOMENCLATURE

a	: scale parameter
b	: transition parameter
d	: details of discrete wavelet transform at resolution 2^{-j}
dp	: particle diameter [mm]
E	: wavelet energy
f	: frequency [Hz]
s	: approximation of discrete wavelet transform at resolution 2^{-j}
U_g	: superficial gas velocity [m/s]
U_l	: superficial liquid velocity [m/s]

$\hat{X}(f)$: Fourier transform of $X(t)$
 $X(t)$: pressure signal in time domain

Greek Letters

Ψ : wavelets, mother wavelet
 ϕ : scaling function

Subscripts

j : multiresolution level
k : time

REFERENCES

Chui, C. K., "An Introduction to Wavelets Vol. 1, Wavelet Analysis and its Applications," Academic Press, San Diego (1992).

Fan, L. S., "Gas-Liquid-Solid Fluidization Engineering," Butterworths Publisher, Boston, MA (1989).

Farge, M., "Wavelet Transforms and Their Applications to Turbulence," *Annu. Rev. Fluid Mech.*, **24**, 395 (1992).

Han, J. H., "Hydrodynamic Characteristics of Three Phase Fluidized Beds," Ph.D. Thesis, Korea Advanced Institute of Science and Technology (1990).

Han, J. H. and Kim, S. D., "Bubble Chord Length Distributions in Three-phase Fluidized Beds," *CES*, **48**, 1033 (1993).

Kang, Y., Woo, K. J., Ko, M. H., Cho, Y. J. and Kim, S. D., "Particle Flow Behavior in Three-Phase Fluidized Beds," *Korean J. Chem. Eng.*, **16**, 784 (1999).

Kim, S. D. and Kang, Y., "Dispersed Phase Characteristics in Three-Phase Fluidized Beds," Encyclopedia of Fluid Mechanics, Mixed-Flow Hydrodynamics - Advances in Engineering Fluid Mechanics Series, **37**, 845 (1996).

Kim, S. H. and Han, G. Y., "An Analysis of Pressure Drop Fluctuation in a Circulating Fluidized Bed," *Korean J. Chem. Eng.*, **16**, 677 (1999).

Kwon, H. W., Han, J. H., Kang, Y. and Kim, S. D., "Bubble Properties and Pressure Fluctuations in Bubble Columns," *Korean J. Chem. Eng.*, **11**, 204 (1994).

Lee, G. S. and Kim, S. D., "Pressure Fluctuations in Turbulent Fluidized Beds," *J. Chem. Eng. Japan*, **21**, 515 (1988).

Lee, S. H., Lee, D. H. and Kim, S. D., "Slug Characteristics of Polymer Particles in a Fluidized Bed with Different Distributors," *Korean J. Chem. Eng.*, **18**(3), 387(2001).

Mallat, S., "A Wavelet Tour of Signal Processing," Academic Press, New York, NY (1998).

Motard, R. L. and Joseph, B., "Wavelet Applications in Chemical Engineering," Kluwer Academic Publishers, Boston (1994).

Otnes, R. K. and Enochson, L., "Applied Time Series Analysis," John Wiley & Sons, NY (1978).

Park, S. H., "Phase Holdups and Pressure Fluctuations in Two- and Three-Phase Fluidized Beds," MS Thesis, Korea Advanced Institute of Science and Technology (1989).

Rioul, O. and Vetterli, M., "Wavelets and Signal Processing," IEEE SP Magazine, **14** (1991).

Wickerhauser, M. V., "Adapted Wavelet Analysis, from Theory to Software," A. K. Peters Publ. (1994).

Wornell, G. W., "Wavelet-Based Representations for 1/f Family of Fractal Processes," Proceedings of the IEEE, **81**(10), 1428 (1993).